



## The positive role of cadmium in TS-1 catalyst for butadiene epoxidation

Mei Wu <sup>a,b</sup>, Huanling Song <sup>a,\*</sup>, Fang Wang <sup>a</sup>, Lingjun Chou <sup>a,\*</sup>

<sup>a</sup> State Key Laboratory for Oxo Synthesis and Selective Oxidation, Lanzhou Institute of Chemical Physics, Chinese Academy of Sciences, Lanzhou 730000, PR China

<sup>b</sup> University of Chinese Academy of Sciences, Beijing 100049, PR China



### ARTICLE INFO

#### Article history:

Received 17 June 2013

Received in revised form 19 August 2013

Accepted 20 August 2013

Available online 28 August 2013

#### Keywords:

Cadmium

Epoxidation

Quantum chemical calculation

Titanium silicalite 1

Vinyloxirane

### ABSTRACT

A series of Cd modified titanium silicalite 1 catalysts with different Cd content ( $x$ Cd-TS-1,  $x = 1\text{--}15$ ) were successfully prepared by ultrasound impregnation. Epoxidation of butadiene over these catalysts were investigated using hydrogen peroxide as oxidant, which indicated that Cd greatly improve the catalytic performance of TS-1 and the selectivity of epoxide. Various characterization methods including quantum chemical calculation were employed to explore the specific roles of Cd in promoting TS-1 catalytic activity. Theoretical calculation consistently suggested Ti–O bond were weakened owing to the introduction of Cd, which resulted in the structure of Cd-TS-1 becoming more relaxant. As a consequence, it is favorable to methanol solvent and  $\text{H}_2\text{O}_2$  interacting with the Ti active site to form five-member transition state during reaction. It was observed that catalysts modified with 1–5 wt% Cd presented both high catalytic activity and good reusability. The highest yield of 0.63 mol/L of vinyloxirane (VO) was obtained, while turnover number (TON, determined as the molar VO obtained per molar Ti atom) could reach to 1466.

© 2013 Elsevier B.V. All rights reserved.

## 1. Introduction

Vinyloxirane (VO) synthesis has attracted more and more attention since its great value to produce high-volume industrial and consumer products [1]. The direct epoxidation of butadiene (BD) provides an excellent pathway for VO preparing. Effective catalysis system for BD epoxidation has been thoroughly studied.  $\text{Ag}/\text{Al}_2\text{O}_3$  [2–4], noble metals [5–7], transition metal oxides [8], along with all kinds of titanium silicalite materials such as TS-1, TS-2, Ti- $\beta$ , Ti-MCM-41/48, and Ti-MWW [9–12] are commonly-used catalysts for olefin epoxidation. Thereinto, TS-1 exhibits remarkable high catalysis efficiency and molecular selectivity. In the report of Zhang et al. [13], BD epoxidation was effectively catalyzed by TS-1. Oxidant and solvent make many differences for various catalysts. TS-1 would perform high activity and selectivity when  $\text{H}_2\text{O}_2$  is applied as oxidant. Moreover,  $\text{H}_2\text{O}_2$  is environmentally benign owing to  $\text{H}_2\text{O}$  as the only by-product. A widely accepted five-membered cyclic structure (a well-defined Clerici-like cycle) mechanism demonstrates that Ti centers in TS-1 are coordinated with the protic solvent and stabilized through hydrogen bonding in the form of Ti-peroxide complex [9,14]. Thus the small electrophilicity and steric

constraints of  $\text{CH}_3\text{OH}$  offers the best medium to the epoxidation of BD [13].

In order to further enhance catalytic reactivity, much attention has been paid on the modification of the TS-1. Alkali and alkaline-earth metals salts with weak basicity have been used as additives to neutralize acid sites in the titanium silicalite, and epoxides selectivity increased markedly [9,15,16]. Arca et al. [17] pre-treated TS-1 with zinc salts, inducing a reduced Ti–OOH electrophilicity and a higher propylene oxide selectivity towards the propylene epoxidation. Also in our previous work [18,19], some incorporated metals in the TS-1 skeletons improved the electrophilicity of active oxygen in the five-member-ring intermediate, and significantly promoted TS-1 catalytic activity for BD epoxidation. However, Zn treated TS-1 exhibited poorer activity for BD epoxidation although VO selectivity increasing slightly. Besides, metals V [20], Nb [21], Zr [22] and Co [23] were also used to modify TS-1 for all kinds of oxidation reactions.

In this work, we have designed kinds of TS-1 catalysts modified by another inexpensive metal Cd for BD epoxidation. Catalysts with different Cd content were prepared by impregnation method. Thereinto, 5Cd-TS-1 showed both excellent activity and durable reusability. In addition, catalytic performance of Cd-TS-1 took good advantage over other metals modifying TS-1 catalysts for the alkene epoxidation, in which  $\text{H}_2\text{O}_2$  utilization was increased 18.1% compared with TS-1. Characterizations by XRD, XPS, BET, FT-IR, UV-vis and quantum chemical calculation were carefully performed, aiming to explore the peculiar roles of Cd in TS-1.

\* Corresponding author. Tel.: +86 931 4968066; fax: +86 931 4968129.

E-mail addresses: [songhl@licp.ac.cn](mailto:songhl@licp.ac.cn) (H. Song), [ljchou@licp.ac.cn](mailto:ljchou@licp.ac.cn) (L. Chou).

## 2. Experimental

### 2.1. Materials and catalysts preparation

$\text{H}_2\text{O}_2$  (40 wt%; local vendor) concentrations were determined by iodometric titration prior to use. Titanium silicalite 1 (TS-1,  $\text{SiO}_2/\text{TiO}_2 = 40$ ) with specific surface area  $463.1 \text{ m}^2/\text{g}$  was from Shanghai Novel Chemical Technology Co. Ltd. Cadmium nitrate ( $\text{Cd}(\text{NO}_3)_2 \cdot 4\text{H}_2\text{O}$ , Shanghai No. 2 Reagent Factory, China) and methanol ( $\text{CH}_3\text{OH}$ , local vendor) were all A.R. grade. All chemicals were used without further purification.

TS-1 catalysts modified with different content of Cd (denoted as  $x\text{Cd-TS-1}$ , where  $x$  stands for CdO mass percent contents:  $x = m_{\text{CdO}}/(m_{\text{CdO}} + m_{\text{TS-1}}) \times 100$ ,  $x$  is in the range of 1–15), were prepared via impregnation method. The typical synthesis process was as follows: 1.00 g of TS-1 was dispersed in distilled water, followed by adding into designed amount of  $\text{Cd}(\text{NO}_3)_2$  solution under vigorous stirring. The mixture was treated under rest for hours and infrared drying until it changed to dry powder. Finally it was further dried up overnight at  $120^\circ\text{C}$ . The output powder was calcined at  $550^\circ\text{C}$  for 6 h.

The regeneration of the 5Cd-TS-1 catalyst was carried out at  $500^\circ\text{C}$  for 4 h.

### 2.2. Physicochemical characterization and computational details

The X-ray powder diffraction analysis (XRD) measurements were performed using an X'Pert Pro multipurpose diffractometer (PANalytical, Inc.) with Ni-filtered  $\text{Cu K}\alpha$  radiation ( $0.15046 \text{ nm}$ ) from  $5.0^\circ$  to  $80.0^\circ$ . Measurements were conducted using a voltage of 40 kV, current setting of 40 mA, step size of  $0.02^\circ$ , and count time of 4 s.

The  $\text{N}_2$  adsorption and desorption isotherms at  $-196^\circ\text{C}$  were recorded on an Autosorb-iQ analyzer (Quantachrome Instruments U.S.). Prior to the tests, samples were degassed at  $200^\circ\text{C}$  for 4 h. The specific surface areas were calculated via the BET method in the relative pressure range of 0.05–0.30; micropore volumes were calculated using adsorption branches of nitrogen adsorption–desorption isotherms by Saito–Foley (SF) methods.

$\text{H}_2$ -TPR was performed on a Zetron–Altamira instrument (AMI-100) employing hydrogen as reducing agent. The samples (0.3 g) were loaded in a U-shaped quartz reactor. Prior to the TPR measurements, samples were pretreated at  $400^\circ\text{C}$  for 30 min in flowing He (50 mL/min) to remove any moisture and other impurities that might be present. After cooling the reactor to  $20^\circ\text{C}$ , a 5%  $\text{H}_2$ –He (50 mL/min) gas mixture was introduced. And then the catalyst was heated to  $900^\circ\text{C}$  at a rate of  $20^\circ\text{C}/\text{min}$  and the hydrogen consumption was measured using an AMETEK (LC-D-200 Dycor AMETEK) mass spectrum.

The oxidation state of Ti and Cd was characterized over a Thermo Fisher Scientific K-Alpha X-ray photoelectron spectroscopy (XPS). The  $x\text{Cd-TS-1}$  powder was pressed to self-supporting wafer prior to analysis.

Fourier transformed infrared spectra (FT-IR) of  $x\text{Cd-TS-1}$  samples were recorded on FT-IR spectrometer (Nicolet Nexus 870) with a resolution of  $4 \text{ cm}^{-1}$  and 64 scans in the region of  $4000$ – $500 \text{ cm}^{-1}$ .

Diffuse reflectance UV-vis spectra (DR UV-vis) was obtained on a PE Lambda 650S spectrometer with  $\text{BaSO}_4$  as standard.

TGA measurements were rendered on a NETZSCH STA 449F3 thermogravimetric analyzer from room temperature to  $900^\circ\text{C}$  at the rate of  $10^\circ\text{C}/\text{min}$ .

Chemical analysis of prepared and used catalysts was done by atomic absorption spectroscopy (AAS) on an ARL 3520 spectrometer.

Ab initio quantum chemical calculations based on the framework of density functional theory (DFT) were performed using

Castep code [24] implemented in Materials Studio 6.0 package of Accelrys. The local density approximation (LDA) of CA-PZ [25,26] with ultrasoft pseudopotential [27] was employed to include the exchange-correlation energy in the total energy. The Kohn–Sham one-electron states are expanded in a plane wave basis set up to a cutoff energy of 300 eV. The criteria for energy and maximum force convergence used are  $2.0 \times 10^{-5} \text{ eV/atom}$  and  $0.05 \text{ eV}/\text{\AA}$ , respectively. All geometries were fully optimized without any constraints. A cluster-like complex, isolated from the TS-1 crystal, having two adjacent rings with 10- and 5-tetrahedral units and inserted in a  $15 \text{ \AA}$  cubic cells was used to investigate the interaction between CdO and Ti-site.

### 2.3. Catalytic evaluation

The epoxidation of BD was performed in a 100 mL stainless-steel autoclave with the magnetic stirrer. Typically,  $0.4 \text{ g } x\text{Cd-TS-1}$  and designed amount of  $\text{H}_2\text{O}_2$  were dispersed in 25.00 mL methanol solvent followed by introducing 0.15 MPa BD. BD was in excess amount during reaction process. The reaction continued for 60 min at  $40^\circ\text{C}$ . Remaining  $\text{H}_2\text{O}_2$  concentration was determined by standard iodometric titration. Chromatography–mass spectroscopy (GC–MS 5973 equipment from Agilent Technology Company) was used to confirm liquid products. VO was confirmed as the main product, and main by-products were small amount of tetrahydro-2-furanmethanol and 4-ethenyl-cyclohexene. Quantities of products were performed on a gas chromatograph (SP-6800A GC) equipped with a flame ionization detector and OV-1701 capillary column. VO yields were determined relating to methanol via external standard method based on the GC results, while concentrations of by-products were too little to determine. VO turnover numbers (TON, determined as the molar VO obtained per molar Ti atom, Eq. (1)), and VO concentrations in the final reaction mixtures were utilized to evaluate activities of different catalysts. Conversions and utilizations of  $\text{H}_2\text{O}_2$  were calculated by means of Eqs. (2) and (3), respectively:

$$\text{TON} = \frac{n_{\text{VO}}}{n_{\text{Ti}}} \quad (1)$$

$$\text{H}_2\text{O}_2 \text{ conversion \%} = 100 \times \left[ \frac{(n_{\text{H}_2\text{O}_2})_0 - (n_{\text{H}_2\text{O}_2})}{(n_{\text{H}_2\text{O}_2})_0} \right] \quad (2)$$

$$\text{H}_2\text{O}_2 \text{ utilization \%} = 100 \times \left[ \frac{n_{\text{VO}}}{(n_{\text{H}_2\text{O}_2})_0} \right] \quad (3)$$

In above equations,  $n_{\text{VO}}$  stands for moles of VO yield after epoxidation reaction;  $n_{\text{Ti}}$  stands for molar of Ti atom in catalyst; besides,  $(n_{\text{H}_2\text{O}_2})_0$  and  $n_{\text{H}_2\text{O}_2}$  stand for the initial molar content and the remaining molar content of  $\text{H}_2\text{O}_2$  after reaction, respectively.

## 3. Results and discussion

### 3.1. Characterization results

#### 3.1.1. XRD characterizations

Crystal structures of TS-1 catalysts with and without Cd were studied by XRD (Fig. 1). All samples possess XRD diffraction patterns identical to those of pure TS-1, confirming the presence of orthorhombic MFI-type crystalline phase [28]. TS-1 samples retain a high degree of crystalline even after Cd doping and calcination. Within the experimental error, a painstaking analysis of  $x\text{Cd-TS-1}$  ( $x=1$ –15) spectra do not disclose free CdO, and other possible Cd oxidic species crystalline phases. This result indicates that CdO particles are highly dispersed on the surface of TS-1 [29]. Moreover, its worth noting that the XRD peak intensities of TS-1 decrease with

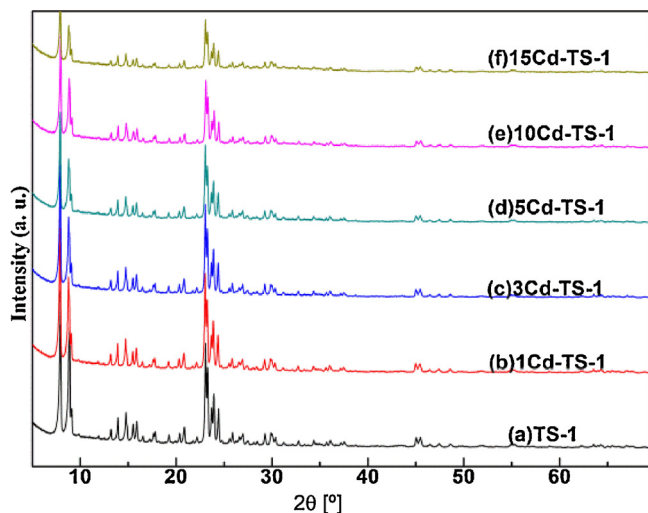


**Fig. 1.** XRD patterns of various  $x\text{Cd-TS-1}$  ( $x=0, 1, 3, 5, 10, 15$ ) catalysts.

the Cd content increasing from 1 to 15 wt%. This may be due to the decrease of the relative amount of TS-1 in the samples as the Cd loading amount increasing [22].

### 3.1.2. $N_2$ absorption and desorption characterizations

The physicochemical properties of  $x\text{Cd-TS-1}$  ( $x=0\text{--}15$ ) catalysts were summarized in Table 1. The surface area and micropore volume of TS-1 decrease with Cd loading increasing. As Cd content increasing from 0 to 15 wt%, they decrease from  $465.2 \text{ m}^2/\text{g}$  and  $0.177 \text{ cm}^3/\text{g}$  to  $341.9 \text{ m}^2/\text{g}$  and  $0.131 \text{ cm}^3/\text{g}$ , respectively. It indicates that Cd oxidic species from the decomposition of cadmium nitrate could block the pore channels and decrease the TS-1 surface area. As a result, excess Cd loading may hinder mass transfer of raw material and product, giving rise to a poor catalytic activity of modified catalysts.

### 3.1.3. $H_2$ -TPR characterizations

As shown in Fig. 2,  $H_2$ -TPR was applied to investigate the interactions between Cd species and TS-1 support. Only one reduction peak presents in every  $H_2$ -TPR curve of various Cd modified samples. It is assigned to the reduction of Cd oxidic species on the surface of TS-1 from the decomposition of cadmium nitrate. The intensity of this reduction peak enhances with the increase of Cd loading, and reaches the maximum for 15Cd-TS-1. As suggested in reference information [30], the top of reduction peak of free CdO should be at  $465^\circ\text{C}$ . The higher reduction temperature of Cd oxidic species supported on TS-1 was observed. Moreover, the reduction temperature rised from  $537^\circ\text{C}$  toward  $650^\circ\text{C}$  with the Cd content increasing from 1 to 15 wt%. It demonstrates that the strong interaction exists between Cd oxidic species and the TS-1 supporter, and the interaction strength was greatly related to Cd loading.

**Table 1**

Physicochemical properties of  $x\text{Cd-TS-1}$  ( $x=0, 1, 3, 5, 10, 15$ ) obtained by BET method.

Cd loading (%)	Surface area ( $\text{m}^2/\text{g}$ )	Micropore volume ( $\text{cm}^3/\text{g}$ )
0	465.2	0.18
1	445.4	0.17
3	419.0	0.16
5	398.3	0.15
10	371.8	0.14
15	341.9	0.13

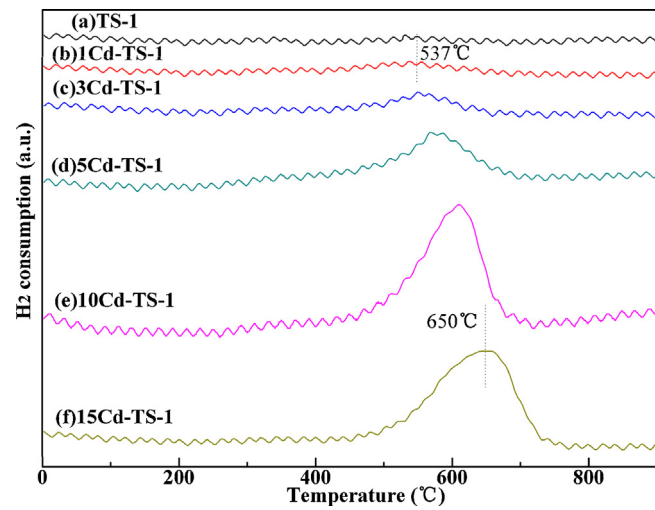


**Fig. 2.**  $H_2$ -TPR profiles for  $x\text{Cd-TS-1}$  ( $x=1, 3, 5, 10, 15$ ) catalysts.

### 3.1.4. FT-IR characterizations

The FT-IR spectra of modified samples, which were exhibited in Fig. 3(a), ranged from  $4000$  to  $500 \text{ cm}^{-1}$ . Band at  $1100 \text{ cm}^{-1}$  with a shoulder at  $1220 \text{ cm}^{-1}$  is attributed to Si—O—Si asymmetric stretching; band at  $803 \text{ cm}^{-1}$  belongs to symmetric stretching/bending of

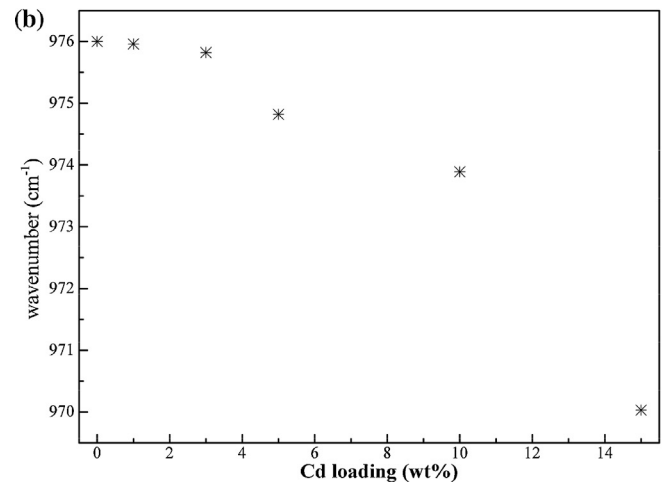
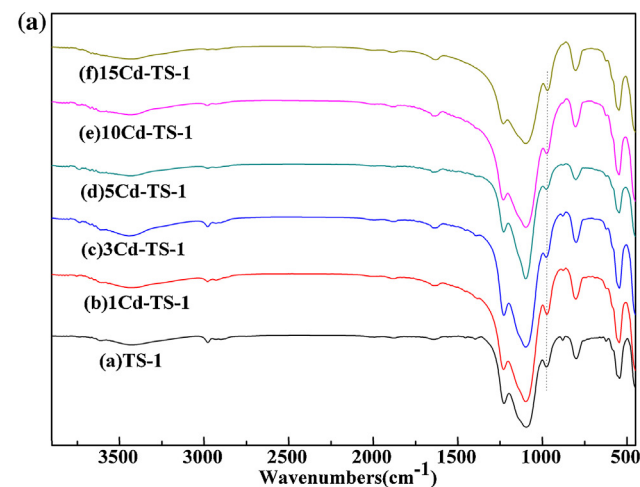


**Fig. 3.** (a) FT-IR spectra of TS-1 modified with different contents of Cd ( $x=0, 1, 3, 5, 10, 15$ ); (b) FT-IR wavenumber decrease around  $970 \text{ cm}^{-1}$  vs Cd loading ( $x=0, 1, 3, 5, 10, 15$ ).

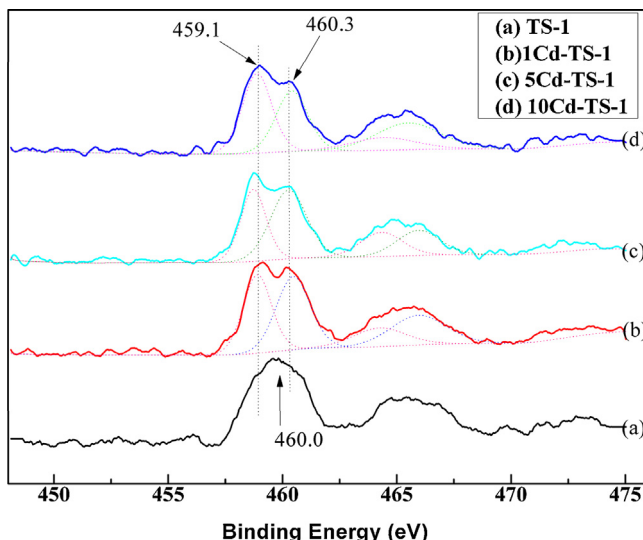


**Fig. 4.** The Ti 2p XPS spectra of the  $x\text{Cd-TS-1}$  ( $x=0, 1, 5, 10$ ) samples.

$\text{SiO}_4$ – $\text{Si}$  bridges; band at  $552\text{ cm}^{-1}$  is assigned to  $\text{Si}=\text{O}=\text{Si}$  rocking [31]. These bands reveal the silica matrix is in a MFI structure, which is in good agreement with the XRD analytical result. Band around  $970\text{ cm}^{-1}$ , which is widely recognized as the stretching mode of the  $[\text{SiO}_4]$  tetrahedral bond with Ti atoms and the fingerprint of framework titanium [22,32,33], appears in all samples. No obvious change in band intensity is disclosed with Cd amount rising. Band migration is observed around  $970\text{ cm}^{-1}$  after the content of Cd increasing. With Cd loading increasing from 0 to 15 wt%, it migrated from  $970.4\text{ cm}^{-1}$  towards  $967.7\text{ cm}^{-1}$  (Fig. 3(b)). The downshift of the stretching vibrational frequency indicated the strength of  $\text{Ti}=\text{O}$  bonds were weakened, which may ascribed to the effect of the doped Cd.

### 3.1.5. XPS characterizations

Fig. 4 displays the XPS spectra of TS-1 samples with different Cd content. The chemical state of titanium was elaborately explored. The Ti 2p<sub>3/2</sub> core-level spectra of reference standard TS-1 show characteristic binding energy at  $460.0\text{ eV}$ , which are assigned to the framework Ti in tetrahedral coordination. For Cd modifying catalysts, two peaks of binding energy at  $460.3$  and  $459.1\text{ eV}$  were clearly observed. The former one can be classified to framework Ti site in the tetrahedral configuration [6]. The later one, which possesses a  $1.2\text{ eV}$  decrease relate to the reference tetrahedral Ti 2p<sub>3/2</sub>, is attributed to framework Ti center with higher coordination number. It can be supposed that the additive Cd coordinates with Ti active site via O, thus makes the Ti coordination number increase. So to that extent, framework  $[\text{Ti}=\text{O}]$  should be weakened due to Cd modification. It was in good agreement with FT-IR results that the peak around  $970\text{ cm}^{-1}$  migrates to lower wavenumber after

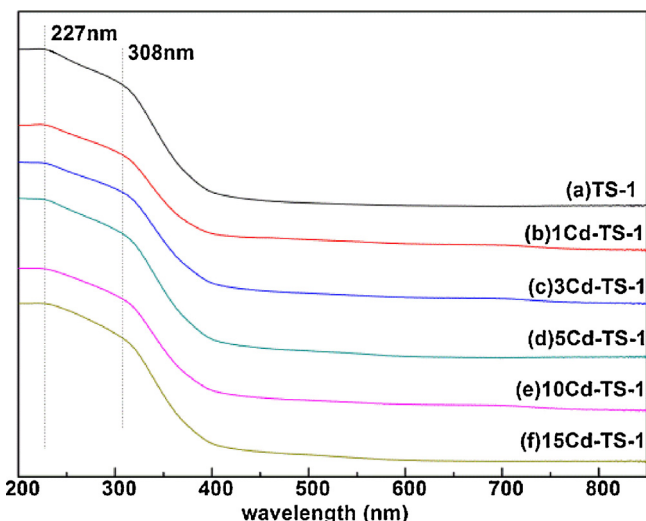


**Fig. 5.** The DR UV-vis spectra of TS-1 with different contents of Cd ( $x=0, 1, 3, 5, 10, 15$ ).

the introduction of Cd. No characteristic peak at  $458.5\text{ eV}$ , which was widely believed as the sign of anatase Ti 2p<sub>3/2</sub> out of TS-1 framework, presented in the XPS spectra of Cd-TS-1 samples.

### 3.1.6. DR UV-vis characterizations

All samples were analyzed by DR UV-vis spectroscopy (Fig. 5), collected in the range of  $200\text{--}850\text{ nm}$ . The local environment of Ti and Cd in  $x\text{Cd-TS-1}$  ( $x=1\text{--}15$ ) were studied. Unmodified TS-1 was still employed as reference sample. To our best knowledge, the absorption peak at  $227\text{ nm}$  is originated from the electronic transfer of the  $\pi\text{-}\pi^*$  transitions between titanium and oxygen in the framework titanium species [34]. It is widely believed as a powerful evidence for the Ti to enter into TS-1 skeleton. Absorption peak at  $308\text{ nm}$  was identified as  $\text{Ti}^{4+}$  ions in an octahedral coordination with two water molecules in the coordination sphere or small hydrated oligomeric  $\text{TiO}_x$  species [35,36]. The absence of absorption of all samples in the range of  $330\text{--}350\text{ nm}$ , which is due either to anatase or to relatively big  $\text{Ti}_x\text{O}_y$  structures, further confirms no anatase or any other extra-framework  $\text{TiO}_2$  phase presents in the Cd-TS-1 samples.

### 3.1.7. Quantum chemical calculation

To evaluate the alteration of geometrical and electronic structure for TS-1 resulting from the modification of Cd, a quantum chemical calculation has been carried out. The optimized geometry of Cd-TS-1 was shown in Fig. 6(a). Table 2 exhibited the calculated atomic charge for Ti, Cd and selected O atoms in TS-1, Cd-TS-1 and CdO.

As can be seen in Fig. 6(a), CdO modified TS-1 via the interaction of O5 with Ti active site. The binding energy (defined as

**Table 2**

Calculated atomic charge for Ti, Cd and selected O atoms in optimized geometries.

Atoms	CdO	TS-1	Cd-TS-1	$\text{CH}_3\text{OH}$	$\text{H}_2\text{O}_2$	I	II
O1	–	-0.980	-1.030	–	–	-0.860	-0.960
O2	–	-0.970	-0.990	–	–	-1.050	-0.930
O3	–	-0.840	-0.890	–	–	-0.870	-0.880
O4	–	-0.970	-0.990	–	–	-0.950	-0.950
O5	-0.70	–	-0.820	–	–	-0.900	–
O6	–	–	–	-0.800	–	-0.680	-0.660
O7	–	–	–	–	-0.560	-0.510	-0.540
O8	–	–	–	–	-0.560	-0.430	-0.490
Ti	–	1.670	1.600	–	–	1.690	1.720
Cd	0.70	–	1.370	–	–	1.350	–

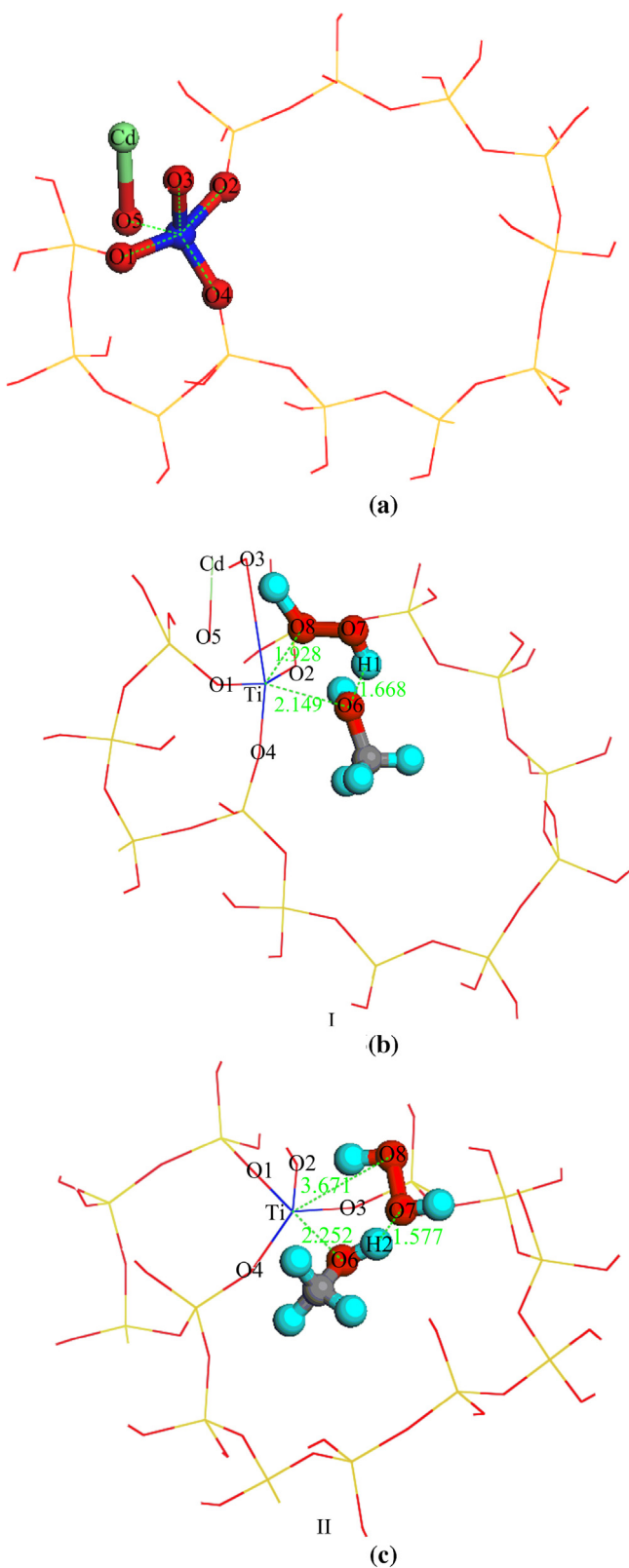


**Fig. 6.** (a) Optimized geometry of Cd-TS-1; (b) optimized geometry of five-membered cyclic intermediate composed of CH<sub>3</sub>OH, H<sub>2</sub>O<sub>2</sub> and CdO-TS-1; (c) optimized geometry of five-membered cyclic intermediate composed of CH<sub>3</sub>OH, H<sub>2</sub>O<sub>2</sub> and TS-1.

**Table 3**

Effect of Cd content on the BD epoxidation (Reaction conditions: 40 °C, 0.15 MPa, 60 min, H<sub>2</sub>O<sub>2</sub> (40 wt%) 0.71 mol/L, xCd-TS-1 0.40 g, CH<sub>3</sub>OH 25.00 mL).

Cd loading (%)	YVO (mol/L) <sup>a</sup>	C <sub>H<sub>2</sub>O<sub>2</sub></sub> (%) <sup>b</sup>	U <sub>H<sub>2</sub>O<sub>2</sub></sub> (%) <sup>c</sup>	TON
0	0.53	86.0	75.2	1238
1	0.61	89.7	85.3	1417
3	0.62	86.0	86.6	1447
5	0.63	80.1	88.8	1466
10	0.55	74.8	77.1	1271
15	0.50	69.7	71.5	1173

<sup>a</sup> VO yield.

<sup>b</sup> H<sub>2</sub>O<sub>2</sub> conversion.

<sup>c</sup> H<sub>2</sub>O<sub>2</sub> utilization.

the energy difference between Cd-TS-1 and the free CdO, TS-1 for CdO on TS-1 is as high as 4.92 eV, which combined with the short Ti-O5 distance (1.792 Å) indicating O5 has coordinated with Ti. It coincided with the XPS results, in which the Ti 2p orbital binding energy decreased from 460.3 eV to 459.1 eV, illustrating Ti coordination number increased. After Cd modification, the length of four Ti–O bonds were found lengthened to 1.820–2.001 Å from 1.776 to 1.795 Å. When comparing the charge distributions on Ti and O atoms in TS-1 and Cd-TS-1, it is observed all of them got electrons after the introduction of CdO, which made the repulsion interaction between Ti and O atoms increase. Both of the lengthened Ti–O bonds and the reduced positive charge on Ti and O atoms suggested the Ti–O bonds were weakened and a more relaxed structure of Cd-TS-1 was formed, which were in good agreement with the results of FT-IR spectra. As a result, more chances are supposed to be provided for CH<sub>3</sub>OH and H<sub>2</sub>O<sub>2</sub> to approach the Ti active site and hence facilitate the formation of five-membered cyclic intermediate.

To confirm this conjecture and get more insight into the catalysis mechanism, a further quantum chemical calculation was carried out to investigate the interaction among Cd-TS-1, CH<sub>3</sub>OH, and H<sub>2</sub>O<sub>2</sub>, denoted as complex I in Fig. 6(b). For comparison, the interaction of CH<sub>3</sub>OH and H<sub>2</sub>O<sub>2</sub> with TS-1 has also been studied, denoted as complex II in Fig. 6(c). As the geometries shown in Fig. 6(b) and (c), it is obviously found that a five-membered cyclic complex was formed between Ti, H<sub>2</sub>O<sub>2</sub> and CH<sub>3</sub>OH. Moreover, the Ti–O<sub>6</sub> distance between Ti and methanol, and Ti–O<sub>8</sub> distance between Ti and hydrogen peroxide, shifted to much shorter ones with the presence of CdO in TS-1, indicating the interaction of CH<sub>3</sub>OH and H<sub>2</sub>O<sub>2</sub> with TS-1 became much stronger after the modification of CdO. Mulliken population analysis about complex I (see Table 2) demonstrated the charges on O<sub>7</sub> and O<sub>8</sub> increased from both –0.560 in free H<sub>2</sub>O<sub>2</sub> to –0.510 and –0.430, respectively, where O<sub>8</sub> is more electron deficient with respect to O<sub>7</sub> and was supposed to react with C=C of BD. When compared complex I with II where TS-1 is not modified by CdO, it is observed that charges on O<sub>7</sub> and O<sub>8</sub> of I are more positive, implying the electrophilicity of O atoms in H<sub>2</sub>O<sub>2</sub> increases when TS-1 is modified by CdO, which is favorable to its electrophilic attack on the double bond of BD.

### 3.2. Effect of Cd loading on BD epoxidation

**Table 3** depicted the results of the BD epoxidation over xCd-TS-1. With the increase of the Cd content, VO yield, H<sub>2</sub>O<sub>2</sub> utilization and TON effectively improved and reached maximum at 5% Cd loading, although the H<sub>2</sub>O<sub>2</sub> conversion gradually decreased. However, higher content of Cd up to 15% resulted in some decline in VO yield, conversion and utilization of H<sub>2</sub>O<sub>2</sub> and TON. Compared with unpromoted TS-1 catalyst, both of H<sub>2</sub>O<sub>2</sub> utilization and TON could increase 18% for Cd-TS-1 catalyst. The results were superior to Ni-TS-1 catalyst in which H<sub>2</sub>O<sub>2</sub> utilization enhanced 15% relative to TS-1. Why Cd has this prominent feature? According to experimental and theoretical results above, the introduction of

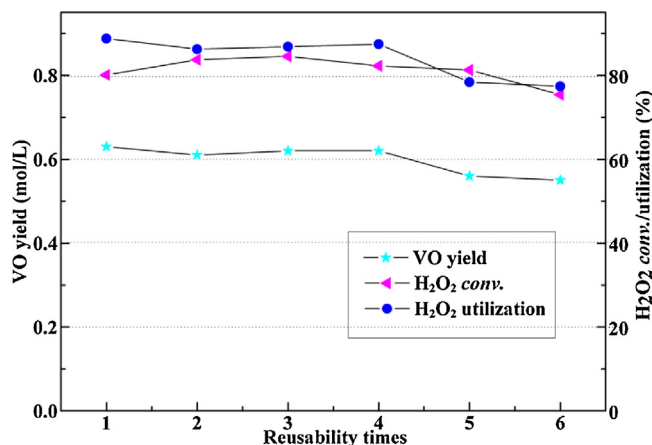


**Fig. 7.** Reusability tests of 5Cd-TS-1 catalyst (Reaction conditions: 40 °C; 0.15 MPa; 60 min; H<sub>2</sub>O<sub>2</sub> (40 wt%) 0.71 mol/L; 5Cd-TS-1 0.40 g; CH<sub>3</sub>OH 25.00 mL).

Cd into TS-1 weakened Ti—O bonds, which were facilely attacked by CH<sub>3</sub>OH and H<sub>2</sub>O<sub>2</sub>. As a result, it is propitious to form the five-membered reaction intermediate. Moreover, electrophilicity of H<sub>2</sub>O<sub>2</sub> in this intermediate was increased. By this token, active O was favorable to be ectrophilic attacked by the double bond of BD. In a word, the roles of Cd coordinating with Ti via oxygen atom played in Ti active site could effectively promote the catalytic performance of TS-1 for BD epoxidation. This positive effect strengthened with Cd loading rising. However, as suggested in the XRD results, the relative TS-1 content in Cd-TS-1 decreased with Cd loading increasing. Also in the N<sub>2</sub> adsorption and desorption results, excess content of Cd would block TS-1 pore channels and decrease the TS-1 surface area. Hence, when Cd content was in excess of 5 wt%, TS-1 activity would be suppressed.

### 3.3. Deactivation and regeneration of 5Cd-TS-1 catalyst

The reusability of 5Cd-TS-1 catalyst was further tested. As Fig. 7 showed, the catalyst kept original activity during four runs: H<sub>2</sub>O<sub>2</sub> conversions and VO yields maintained above 80% and 0.6 mol/L, respectively. However, VO yield and H<sub>2</sub>O<sub>2</sub> utilization decreased in the fifth repeated reaction. In order to clarify this phenomenon, the fresh and used catalysts were characterized by TGA, N<sub>2</sub> adsorption and desorption and AAS. TGA patterns of fresh or used 5Cd-TS-1 catalysts were shown in Fig. S1. No exothermic peak appeared for the fresh catalyst as Fig. S1(a) shown. While after 6 runs reaction, a small exothermic peak (Fig. S1(b)) accompany with the weight loss of 6.79% appeared around 420 °C. It implied that organic compound, which could deposit in the pore channel and overlay Ti active sites, was absorbed by TS-1 support during reaction. It was confirmed by the BET analysis results (Table S1), in which the surface area of 5Cd-TS-1 catalyst dropped from 398.3 m<sup>2</sup>/g to 319.2 m<sup>2</sup>/g after six repeated reaction, and also the micropore volume decreased from 0.152 cm<sup>3</sup>/g to 0.126 cm<sup>3</sup>/g. With regeneration runs increasing, the residua of organic compound will be more and more difficult to clear up. Deposited organic compound would reduce the mass transfer efficiency for the reaction system, inducing the deactivation of the catalyst. In addition, Cd and Ti contents of the fresh and used 5Cd-TS-1 catalysts were compared by AAS. As we can see from Table S1, Cd content decreased from 3.39% in fresh catalyst to 2.47% in used one, and 0.98 ppm of Cd was detected in the sixth reacting solution. It suggested tiny Cd leached during the repeated reactions. Whereas, the content of Ti, with lower than 0.5 ppm in the sixth reacting solution, has no clear change after six repeated reaction. It demonstrated that Ti loss was not the main reason for catalyst deactivation.

## 4. Conclusions

Cd modified TS-1 catalysts were employed to catalyze butadiene epoxidation for vinyloxirane. TS-1 catalytic activities were significantly promoted with 1–5 wt% content of Cd. The special modification effect was responsible for the coordination of additive Cd with Ti center via O atom. It leaded to the formation of a more relaxed Cd-TS-1. As a result, more chances were provided for CH<sub>3</sub>OH and H<sub>2</sub>O<sub>2</sub> to approach the Ti active site. It had been testified that O of H<sub>2</sub>O<sub>2</sub> close to Ti in five-membered intermediate was activated with promoted electrophilicity by Cd modification. Therefore, double bond electrophilic epoxidation of butadiene would be facilely. 5Cd-TS-1, which presented promising reusability and high catalytic activity, was turned out to be an ideal candidate catalyst for butadiene epoxidation.

## Acknowledgement

The authors sincerely acknowledge the financial support from the National Natural Science of China (Grant No. 21133011, 21203218).

## Appendix A. Supplementary data

Supplementary data associated with this article can be found, in the online version, at <http://dx.doi.org/10.1016/j.molcata.2013.08.019>.

## References

- [1] E. Doskocil, G. Mueller, J. Catal. 234 (2005) 143–150.
- [2] J.W. Medlin, M.A. Barreau, J.M. Vohs, J. Mol. Catal. A: Chem. 163 (2000) 129–145.
- [3] H.L. Song, G. Chen, S.B. Li, et al., React. Kinet. Catal. Lett. 85 (2005) 45–49.
- [4] J. Monnier, J. Catal. 226 (2004) 321–333.
- [5] J.J. Bravo-Suarez, K.K. Bando, T. Fujitani, et al., J. Catal. 257 (2008) 32–42.
- [6] C. Shi, B. Zhu, M. Lin, et al., Eur. J. Inorg. Chem. 2009 (2009) 4433–4440.
- [7] V.R. Choudhary, D.K. Dumbre, Top. Catal. 52 (2009) 1677–1687.
- [8] V. Choudhary, R. Jha, P. Jana, Catal. Commun. 10 (2008) 205–207.
- [9] M.G. Clerici, P. Ingallina, J. Catal. 140 (1993) 71–83.
- [10] S. Krijnen, P. Sánchez, B.T.F. Jakobs, et al., Microporous Mesoporous Mater. 31 (1999) 163–173.
- [11] L. Wang, Y. Liu, H. Zhang, et al., Chin. J. Catal. 27 (2006) 656–658.
- [12] A. Wroblewska, A. Fajdek, J. Wajzberg, et al., J. Adv. Oxid. Technol. 11 (2008) 468–476.
- [13] X.M. Zhang, Z.R. Zhang, J.S. Suo, et al., Catal. Lett. 66 (2000) 175–179.
- [14] X. Liu, X. Wang, X. Guo, et al., Catal. Today 93–95 (2004) 505–509.
- [15] G. Li, X.S. Wang, H.S. Yan, et al., Appl. Catal., A: Gen. 218 (2001) 31–38.
- [16] C.V. Rode, U.N. Nehete, M.K. Dongare, Catal. Commun. 4 (2003) 365–369.
- [17] V. Arca, A. Boscolo Boscoletto, N. Fracasso, et al., J. Mol. Catal. A: Chem. 243 (2006) 264–277.
- [18] M. Wu, L. Chou, H. Song, Catal. Lett. 142 (2012) 627–636.
- [19] M. Wu, L. Chou, H. Song, Chin. J. Catal. 34 (2013) 25–33.
- [20] S. Chen, S. Wang, X. Ma, et al., Chem. Commun. 47 (2011) 9345–9347.
- [21] D. Prasetyoko, Z. Ramli, S. Endud, et al., Mater. Chem. Phys. 93 (2005) 443–449.
- [22] D. Prasetyoko, Z. Ramli, S. Endud, et al., J. Mol. Catal. A: Chem. 241 (2005) 118–125.
- [23] J. Jiang, R. Li, H.L. Wang, et al., Catal. Lett. 120 (2008) 221–228.
- [24] M.D. Segall, P.J.D. Lindan, M.J. Probert, et al., J. Phys.-Condens. Matter 14 (2002) 2717–2744.
- [25] D.M. Ceperley, B.J. Alder, Phys. Rev. Lett. 45 (1980) 566–569.
- [26] J.P. Perdew, A. Zunger, Phys. Rev. B 23 (1981) 5048–5079.
- [27] D. Vanderbilt, Phys. Rev. B 41 (1990) 7892–7895.
- [28] T. Armaroli, F. Millella, B. Notari, et al., Top. Catal. 15 (2001) 63–71.
- [29] Q.H. Tang, Q.H. Zhang, H.L. Wu, et al., J. Catal. 230 (2005) 384–397.
- [30] B.M. Abu-Zied, A.M. El-Awad, J. Mol. Catal. A: Chem. 176 (2001) 227–246.
- [31] M. Capel-Sánchez, Appl. Catal. A: Gen. 246 (2003) 69–77.
- [32] S. Bordiga, A. Damin, F. Bonino, et al., J. Phys. Chem. B 106 (2002) 9892–9905.
- [33] G. Ricchiardi, A. Damin, S. Bordiga, et al., J. Am. Chem. Soc. 123 (2001) 11409–11419.
- [34] J. Zhuang, D. Ma, Z. Yan, et al., Appl. Catal. A: Gen. 258 (2004) 1–6.
- [35] X.S. Wang, X.W. Guo, G. Li, Catal. Today 74 (2002) 65–75.
- [36] H. Li, Q. Lei, X.M. Zhang, et al., Microporous Mesoporous Mater. 147 (2012) 110–116.